The INE-Beamline for actinide research at ANKA

By J. Rothe[1], M. A. Denecke[1,*], K. Dardenne[1] and Th. Fanghänel[1,2]

[1] Forschungszentrum Karlsruhe, Institut für Nukleare Entsorgung, P.O. Box 3640, 76021 Karlsruhe, Germany
[2] Physikalisch-Chemisches Institut, Universität Heidelberg, Im Neuenheimer Feld 253, 69120, Heidelberg, Germany

X-ray absorption spectroscopy / Nuclear waste disposal / Actinide speciation / Multi-purpose beamline

Summary. The Institut für Nukleare Entsorgung (INE) at the Forschungszentrum Karlsruhe (FZK), Germany, has constructed and is operating a beamline at the synchrotron source ANKA dedicated to actinide speciation investigations related to nuclear waste disposal as well as applied and basic actinide research. Experiments on nuclides not suited as nuclear fuel with activities up to 10^6 times the limit of exemption inside a safe and flexible containment concept are now possible. The design is for a multi-purpose beamline, *i.e.*, a number of methods (XAFS, surface sensitive and spatially resolved techniques) are envisaged on one and the same sample, with X-ray energies from 2472 eV (S K edge) to 23 220 eV (Rh K edge). The commissioning of the INE-Beamline was officially completed in September 2005 and meanwhile regular user operation has been started. Here we present a description of this new facility and examples for X-ray absorption studies on actinides and homologues performed during the beamline commissioning phase.

Introduction

The Institut für Nukleare Entsorgung (INE) at the Forschungszentrum Karlsruhe (FZK), Germany, has constructed and commissioned a beamline dedicated to actinide research [1] at the FZK synchrotron source ANKA. Official operation of the INE-Beamline commenced on October 1st, 2005. There is presently a growing demand for synchrotron facilities, where the infrastructure, safety equipment, and expertise are available for performing research on radioactive samples. One great advantage of the INE-Beamline is that the ANKA accelerator and INE's active laboratories are both located within the same FZK site. This symbiosis has numerous advantages including profiting from the existing infrastructure, backed by decades of know-how. Samples can be prepared, characterized, and analyzed using the spectroscopic, analytical, microscopic, and structural methods available at INE's active laboratories before being transported to ANKA and investigated using synchrotron based methods at the INE-Beamline. The time-span between sample preparation and experiment is relatively short, which allows investigations of dynamic systems within

a time-frame of hours. The samples are also retrievable, so that sample characterization in INE laboratories following the experiments at the INE-Beamline is possible. In addition, hazards associated with transporting radioactive samples to and from INE and nearby ANKA are minimized and the administrative requirements associated with such transports simplified. In the following we present a discussion of the design considerations of the INE-Beamline, a short description of the ANKA facility, beamline optical components, experimental equipment available, and first results of commissioning measurements made beginning in August 2004.

INE-Beamline design considerations

The research and development at INE is largely aimed at safety assessment of proposed deep geological repositories for high-level, heat producing nuclear waste disposal. To ensure valid performance safety assessment, a molecular understanding of processes determinant in the fate of radionuclides, notably the actinides, is essential. To this end, the major portion of research at INE is concerned with actinide speciation, including coordination and redox chemistry of actinides, actinide solubility, determination and characterization of actinide cations sorbed onto surfaces (*e.g.*, at the mineral-water interface), investigation of actinide containing precipitates, colloids, and secondary phases, as well as glass and spent fuel corrosion. Because actinide speciation associated with nuclear disposal concerns is manifold, the major aim in the INE-Beamline design is to ensure variability, *i.e.*, provide a multi-purpose station, where a number of methods are possible. The methods available are standard, surface sensitive, and spatially resolved methods. The standard X-ray methods X-ray absorption fine structure (XAFS) and X-ray fluorescence (XRF) are available and it will be possible in the future to combine XAFS with X-ray diffraction (XRD). Because many reactions of actinides in the hydro- and geo-sphere are at interfaces and junctions, emphasis at the INE-Beamline is being placed on surface sensitive techniques based on grazing incidence (GI) geometry such as GI-XAFS, X-ray reflectivity, and total external reflection X-ray fluorescence analysis (TXRF). In addition, a micro-focus option will be available after a planned future upgrade to offer spatially resolved measurements. This will allow chemical state imaging (μ-XAFS),
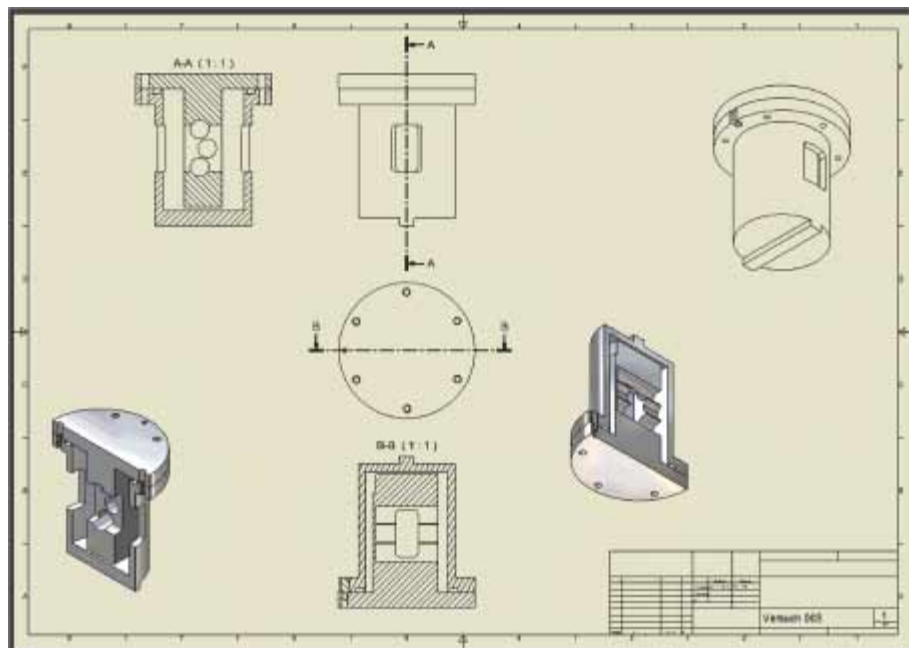
Fig. 1. Blue print of the standard transmission sample holder. Lid diameter = 90 mm. The design example is for wet paste or liquid samples sealed in 2 ml vials (design by G. Herrmann, INE workshop).

elemental mapping (μ-XRF), and identification of phases (μ-XRD). The combination of X-ray methods with other techniques, *e.g.*, laser based methods, will be possible at the beamline.

Investigation of samples with activities up to 10^6 times the limit of exemption of nuclides not suited as nuclear fuel are possible. This amount of activity allows experiments on samples containing, *e.g.*, more than 25 mg long-lived nuclides ^{237}Np, ^{242}Pu, ^{243}Am, or ^{248}Cm. The necessary infrastructure and safety equipment is available at the INE-Beamline for active experiments. The experimental section of the radiation hutches is equipped with a special ventilation/filter system, specially sealed chicanes, easily decontaminated surfaces, and a personnel lock room with a hand-foot monitor for entry and exit. During the experiments, the samples themselves are contained within two independent levels of containment. The concept ensures highest flexibility; there is no predetermined container geometry. The sample primary containment depends on the sample properties (solid, liquid or wet paste) and the secondary containment is the sample holder itself. The first containment is typically a sealed sample cuvette, vial, or plastic bag. The standard second containment is a mechanically stable cylinder having sealed windows for beam entrance, transmitted beam and fluorescent beam, into which a sample or a number of samples are mounted (Fig. 1). The cylinder is placed onto a motorized stage allowing remote-controlled sample changing and positioning relative to the less than mm-sized incident beam. The windows are made of low-Z material, *e.g.*, Kapton® or polycarbonate. Special sample containers for non-standard geometries (*e.g.*, for GI-XAFS) are available or can be easily adapted to the experimental requirements. A special protocol for working with radioactive samples at the INE-Beamline exists and must be adhered to. Neither active chemistry on radioactive samples, nor investigations on nuclear fuel material such as ^{239}Pu are presently permitted at the INE- Beamline. However, these are options for a future license extension.

The ANKA light source

The ANKA storage ring is operated at 2.5 GeV, with a characteristic energy of ~ 6.0 keV, and presently a beam current of ~ 200 mA. The ring is usually refilled twice a day. The beam lifetime ranges from 15 to 30 h. The overview of the ANKA light source with the accelerator components and the beamlines installed in the 60×60 m^2 experimental hall is depicted Fig. 2. More information can be found
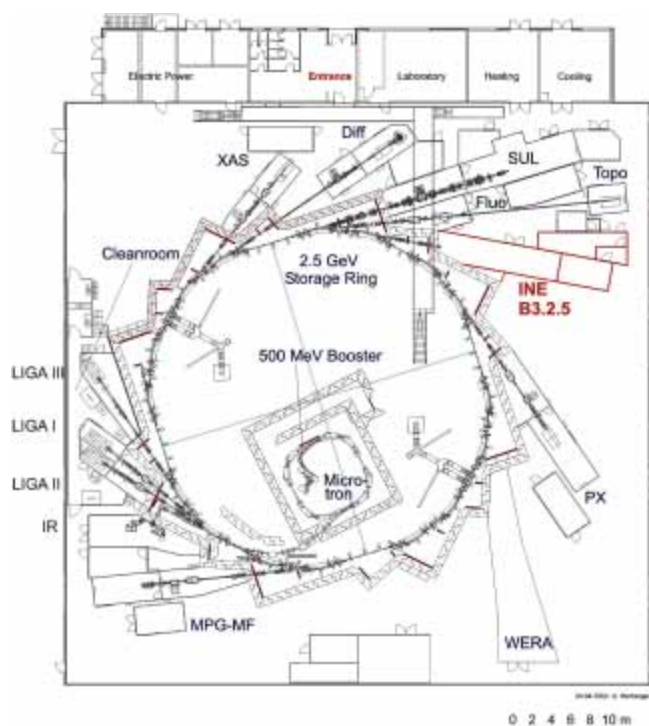

Fig. 2. Overview of the ANKA light source with its storage ring and the beamlines installed in the 60×60 m^2 hall. The location of the INE-Beamline (port B3.2.5) is indicated on the right. The outline of the INE-Beamline hutches and cabins are shown.

at the ANKA web-site [2]. The INE-Beamline is located at the bending magnet (BM) port designated 3.2.5 at the east side of the building. The envelope of the radiation protection hutches and the control cabin with integrated lock room bordering the experimental hutch is also shown in Fig. 2.

INE-Beamline optics and experimental station

The layout scheme of the INE-Beamline is given in Fig. 3. The INE-Beamline design is optimized for X-ray spectroscopic investigations using photon energies from the K-edge of S (2472 eV) to the Rh K-edge (23 220 eV). This range covers key energy regions of interest for investigations of actinides (L_3-edges $\sim$ 16–20 keV) and lanthanides, as actinide homologues and for comparative studies (L-edges $\sim$ 5.5–11 keV). The thickness of the Be window separating the beamline vacuum from the first mirror and ring vacuum is the determinant factor for the lower energy limit. Presently the Be window is 100 μm thick. Future replacement with a 50 μm window may render P K-edge experiments possible. The upper energy is limited by both the Rh coating on the mirrors and the characteristic energy of the ANKA ring. The monochromator at the INE-Beamline is a Lemonnier type double-crystal X-ray monochromator (DCM), built at the Universität Bonn, Physikalisches Institut, with INE contributing the first crystal copper cooling block and second crystal piezo actuator adjustment for detuning and feedback control to maintain constant content of harmonic radiation. The pressure inside the DCM vacuum housing is $\sim 10^{-6}$ mbar and the housing is only 380 mm in diameter, allowing fast changes of crystals, without long pumping times. Four pairs of crystals are presently available, Si(111), Si(311), Ge(220), and Ge(422). The DCM can also accommodate multi-layer mirrors for wide energy band-pass experiments, *e.g.*, for XRF analysis measurements requiring higher flux.

The beamline optics includes collimating and focusing Rh coated silicon mirrors for a mm beam dimension at the sample position. The synchrotron radiation beam is vertically collimated through the cylindrical mirror (Mirror 1) up-stream from the DCM. Down-stream from the DCM, the beam is focused horizontally and vertically by a toroidal mirror (Mirror 2). Mirror 2 is suspended hanging so that the beam is reflected down from its surface, in order to allow studies of liquid films. The beam focus location is in the experimental hutch at a distance of $\sim$ 24 m from the BM source. There is a beam-shutter between the experimental

and optics hutches so that work can be performed in the experimental hutch without having to turn off the beam in the optics hutch, thereby keeping optical elements under a constant heat load. The distance between Mirror 2 and the beam focus is as nearly the same distance from the source to Mirror 2 as possible, thereby minimizing source point image aberration. In order to enable spatially resolved studies with a μ-focused incident beam, an upgrade is planned to install an auxiliary μ-focusing optic such as a polycapillary, an elliptical monocapillary, or planar compound refractive lenses (CRL) fabricated by the Institut für Mikrostrukturtechnik (IMT) at FZK [3]. The focal length of monocapillaries and CRLs can be a number of centimeters, which is an advantage for working with radioactive samples where their containment limits the working distance between focusing optics and sample. Capillaries have the advantage for spectroscopy in that they are achromatic. No achromatic CRL is yet available, although design studies for achromatic planar CRLs are presently being conducted at IMT.

The optical tabletop in the experimental hutch is a 1.2×3 m^2 breadboard, large enough to accommodate almost any experimental set-up. Three ionization chambers (HASYLAB Design, "IONIKA") and a LEGe five pixel fluorescence detector (Canberra) are available for recording XAFS spectra in transmission and fluorescence mode. The grazing incidence equipment (HUBER Diffraktionstechnik GmbH) available at the beamline consists of two goniometer cradles with a common center of rotation (step-size = 0.0001°), a z-stage (step-size = 40 nm) and a rotation stage (step-size = 0.0001°), as well as two micrometer-adjustable vertical slits. The goniometer cradles are for adjusting the relative incident angle of the impinging beam onto the sample surface, the z-stage for vertical height adjustment, and the rotational stage for selecting the sample surface orientation relative to the synchrotron beam polarization vector during polarization dependent measurements. There is a special chamber available at the beamline for performing spectroscopy measurements at lower energies.

Beamtime request

The INE-Beamline and INE active laboratories are one of the pooled facilities of the EU European Network of Excellence for Actinide Sciences (ACTINET) and access to the beamline is possible *via* this avenue. A portion of annual beamtime at the INE-Beamline (30%) is available *via* the standard ANKA facility proposal procedure (for detailed
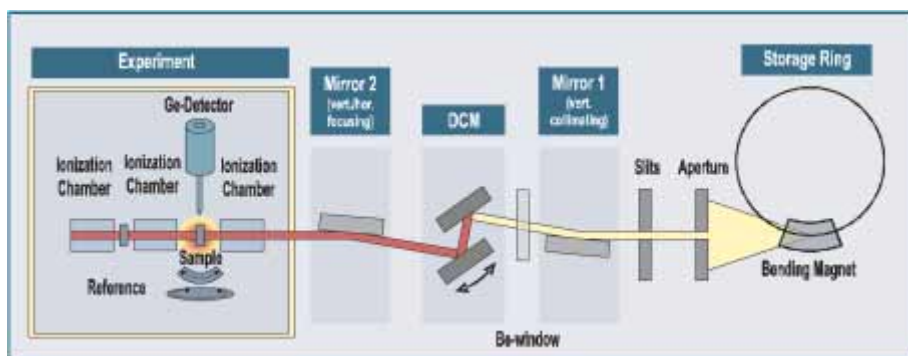

Fig. 3. Layout scheme of the INE-Beamline installed at ANKA port 3.2.5. The experimental hutch marked with a rectangular box is operated as controlled area, where experiments on radioactive samples are allowed.

information see [2]). ACTINET users are prompted to also submit a proposal to the ANKA facility for their beam-time. Experiments are also possible through cooperation with INE. INE-Beamline scientists are to be contacted prior to proposal submittal to ensure feasibility of any experiment involving radioactivity (contact persons can be found in [4]). INE provides a radiation protection officer during active measurements who is responsible for all radioactive substances.

XAFS investigations performed during the commissioning phase

First X-ray absorption measurements including extended X-ray absorption fine structure, EXAFS, spectra of reference foils in the actinide and lanthanide L_3 energy range were recorded in August 2004. The first transport of radioactive samples to the beamline and subsequent X-ray absorption measurements were performed with americium (^{243}Am) containing samples on February 17, 2005 (see example (ii) below). In the following we report on selected examples of on-going research projects performed during the commissioning phase of the INE-Beamline.

(i) XAFS investigation of the formation and structure of Zr(IV) colloids

Due to its reported similar hydrolysis and colloid chemistry, Zr(IV) serves as a homologue for Pu(IV) [5]. We have characterized the structure of the Zr(IV) aqueous solution species at low pH and the species upon increasing pH across the solubility limit (1.0 to 3.3) in a coulometric titration. Our recent results using laser induced breakdown detection and UV-Vis spectroscopy suggest that a micro-crystalline phase of very small size exists at low pH; at higher pH larger, less ordered Zr(IV) colloids exist and these determine the solubility of amorphous Zr(OH)$_4$. Analysis of EXAFS data shows the structure of the micro-crystalline colloids in a 0.1 mol l^{-1} Zr aqueous solution at low pH (0.2) to contain tetrameric units, similar to those in ZrOCl$_2 \cdot$8H$_2$O. Characterization of the coulometric titration solutions by means of EXAFS shows that oligomeric species form as the solubility limit is approached (Fig. 4). None of the spectra for samples with pH 2 and higher resemble that for monoclinic ZrO$_2$, the stable colloids at pH 0.2 or the starting solution at pH 1. We conclude that the Zr in these titration samples must have a different structure. The structure of these solution species is not a simple ZrO$_2$; it has neither the monoclinic, cubic, orthorhombic, nor tetragonal ZrO$_2$ structure. Its structure also cannot be derived from simple stacking of tetrameric [Zr$_4$(OH)$_8$(H$_2$O)$_{16}$]$^{8+}$ units. The Zr−O coordination number (N) of the polynuclear species in the samples with pH $\geq$ 2 is near eight and its distance shows little variation. At the same time, the Fourier transform (FT) Zr−Zr peak is relatively small and likely contains more than one distance. We interpret these results as indicating that the species are built up of primarily ZrO$_8$ building blocks, but the associated Zr sublattice is highly disordered. Polymerization and packing into a more condensed system is likely leading to a disordered and defect-rich Zr sublattice. The data shown here represents
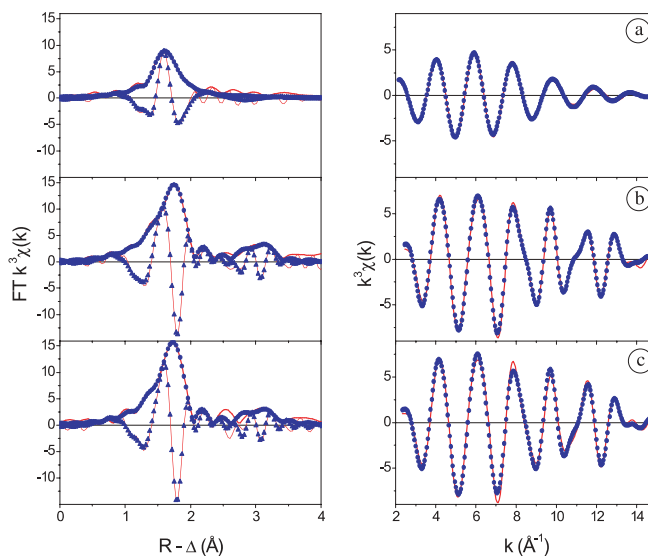

Fig. 4. ZrK EXAFS of (**a**) partially hydrolyzed Zr(IV) at pH 1 (no Zr−Zr peak visible), (**b**) formation of Zr$_x$(OH)$_y^{4x-y}$ oligomers at pH 2.0, and (**c**) approaching Zr(IV) solubility limit (formation of > 5 nm particles) at pH 2.8. Left panel: FT magnitude of EXAFS data (solid line), fit magnitude (circles), FT imaginary part (thin solid line) and fit imaginary part (triangles). Right panel: k^3-weighted back-transformed fit (circles) and corresponding Fourier-filtered data (solid line).

part of the first comprehensive series of samples measured at the INE-Beamline in October 2004 [6].

(ii) XAFS investigation of Am(III) incorporation into secondary minerals

Radionuclide interaction with minerals (*e.g.*, adsorption and structural incorporation) strongly affects their transport properties in aqueous media. The focus in this study is on the interaction of trivalent americium with secondary minerals, calcite and iron oxy/hydroxide (HFO), which possibly form upon container or waste matrix corrosion. Fig. 5a depicts the Am L_3 X-ray absorption near edge structure, XANES, of the Am^{3+} aquo ion, a HFO sorption species, and the latter after one month of tempering [7]. Comparing the energy difference (ΔE) between the major XANES features [8] reveals that the Am−O shell of the tempered transformation species has shorter bonds than those in the Am^{3+} aquo ion and in the sorption species. ΔE is the same, *i.e.*, the bond lengths are the same in the Am^{3+} aquo ion and sorption species; this is corroborated from their EXAFS (not shown). The Am L_3 EXAFS for calcite crystals doped with Am(III), prepared in a mixed-flow-reactor under constant and controlled conditions, is shown in Fig. 5b. The Am−O distance obtained from EXAFS analysis of this data (5–6 O atoms at 2.40 Å) is in good agreement with the structural parameters observed for rare-earth element doped calcite [9, 10]. In both the HFO and calcite systems actinide incorporation into the mineral phases is inferred.

(iii) Interaction of U(VI) with silica and aluminosilicate colloids

Aquatic colloids, *e.g.*, aluminosilicate colloids, are ubiquitous in natural water [11]. Actinide ions of high charge interact with aquatic colloids, generating colloid-borne actinides.
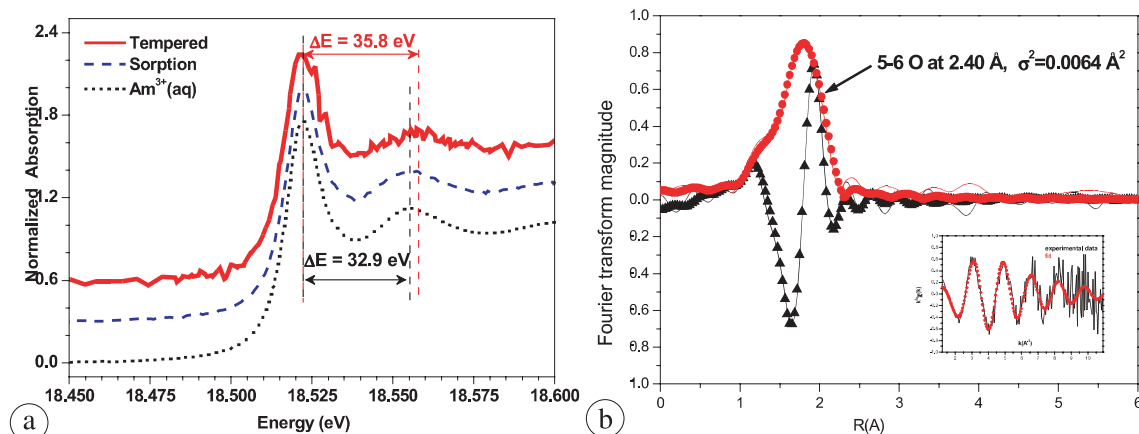
Fig. 5. (a) Am L_3 XANES of the Am^{3+} aquo ion, the HFO sorption species, and the latter after one month tempering; (b) Am L_3 edge k^2-weighted EXAFS (insert) and corresponding FT recorded for Am^{3+} doped calcite. Experimental data shown as lines and fit function as symbols.

Colloids therefore may play a carrier role for actinide migration in natural aquifer systems without substantial geochemical hindrance. Hydroxyaluminosilicate (HAS) colloids are candidates capable of serving as such vehicles for colloid-mediated transport. HAS colloids form by co-precipitation of silicic acid with dissolved aluminium ions and/or aluminium hydroxide species and are assumed to be precursors of natural aluminosilicates. For studying their interaction with actinides, co-precipitation experiments are performed in the presence of trace amounts of actinides [12]. In this example, U(VI) species incorporated into silica and aluminosilicate colloids are characterized by U L_3 EXAFS measurements (Fig. 6). Similar to our earlier EXAFS work on Eu(III) incorporation into silica and HAS colloids, backscattering from the second neighbor Al/Si shell is clearly observed, with a total coordination number, N(Si/Al), of ~ 3. No more than one Si atom is reported for surface-bound uranyl silicate complexes [13, 14]. These findings lead to the conclusion that U(VI) is incorporated into the colloid structure.

(iv) PuL_3 XAFS investigation of colloidal Pu(IV)-fulvate species

After the decay of the shorter lived fission products, the long-lived actinides, plutonium in particular, dominate the radiotoxicity of disposed nuclear fuel. For a reliable risk assessment of nuclear waste disposal in deep geologic formations, understanding of the processes which control plutonium migration behaviour is indispensable. Our present understanding of plutonium chemistry at conditions found in deep geological underground repositories remains unsatisfactory. Especially the oxidation state of plutonium plays a crucial role in its migration behaviour [15]. The influence of a natural fulvic acid (FA), GoHy-573, on plutonium speciation is investigated using XAFS. During this first measurement of plutonium samples at the INE-Beamline, three samples of ^{242}Pu are investigated at different FA concentrations and contact times (Fig. 7a). Significant differences in XANES features between samples are observed (Fig. 7b). While all spectra show a similar first inflection point at about 18.062 keV, the shoulder positioned to the right of the main absorption feature or white line (WL) at $\sim 18\,075$ eV observed in the XANES for sample 1 is indicative of the $Pu^VO_2^+$ dioxo or plutonyl cation. Sample 3 does not exhibit this plutonyl feature and its XANES is typical for Pu(IV). The normalized WL intensity in this sample is slightly decreased compared to the Pu^{4+} aquo ion spectrum. The normalized area of the WL for both spectra remains constant, however. This is indicative of Pu(IV) oxohydroxide colloidal species formation [16]. Sample 2 represents a mixture of the two species, PuO^{2+} and colloidal Pu(IV).
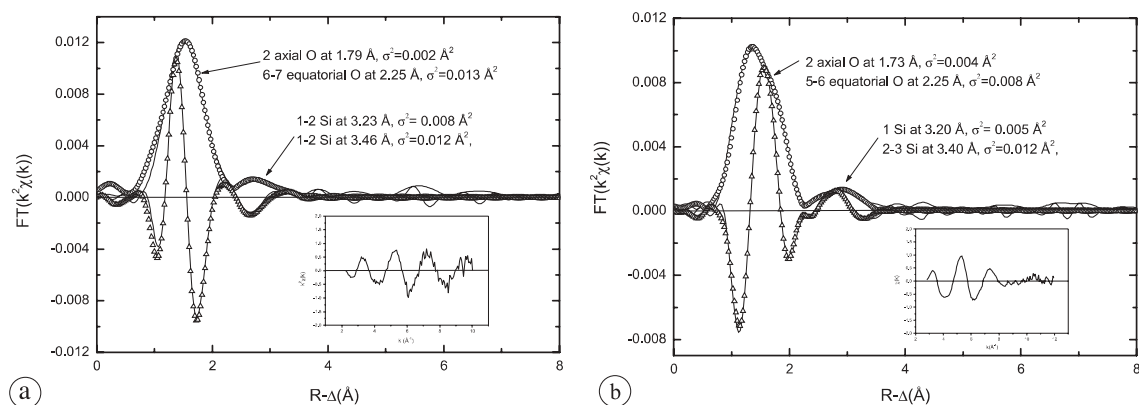

Fig. 6. (a) U L_3 edge k^2-weighted EXAFS (insert) and corresponding FTs for U(VI) incorporated into silica. (b) EXAFS (insert) and corresponding FTs for U(VI) incorporated into HAS colloids. Theoretical fits are depicted as (symbols). Both FT and imaginary part are shown.
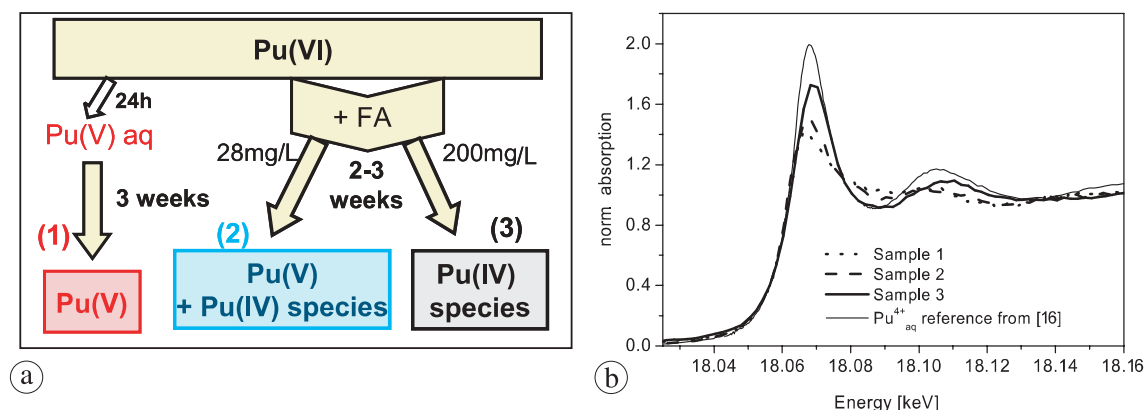
Fig. 7. (**a**) Investigation of Pu(VI) speciation change after addition of a natural fulvic acid (GoHy-573); (**b**) Normalized Pu L_3 XANES of samples 1–3 and Pu^{4+} aquo ion reference. Sample (1) XANES is indicative of the $Pu(V)O_2^+$ ion and the XANES of sample (3) is typical for Pu(IV) oxo/hydroxide colloidal species. Sample (2) represents a mixture of these two species.

References

1. Denecke, M. A., Rothe, J., Dardenne, K., Blank, H., Hormes J.: *The INE-Beamline for Actinide Research at ANKA*. Physika Scripta T115, 1001 (2005).
2. http://ankaweb.fzk.de/
3. Nazmov, V., Reznikova, E., Somogyi, A., Mohr, J., Saile, V.: Planar sets of cross X-ray refractive lenses from SU-8 polymer. Proc. SPIE **5539**, 235 (2004).
4. http://ankaweb.fzk.de/instrumentation_at_anka/beamlines.php?id=9&field=7.
5. Hummel, W., Berner, U., Curti, E., Pearson, F. J., Thoenen T.: Nagra/PSI chemical thermodynamic data base 01/01. Radiochim. Acta **90**, 805 (2002).
6. Cho, H.-R., Walther, C., Rothe, J., Neck, V., Denecke, M. A., Dardenne, K., Fanghänel, Th.: Combined LIBD and XAFS investigation of the formation and structure of Zr(IV) colloids. Anal. Bioanal. Chem. **383**, 28 (2005).
7. Dardenne, K., Schäfer, T., Lindqvist-Reis, P., Denecke, M. A., Plaschke, M., Rothe, J., Kim J. I.: Low temperature XAFS investigation on the lutetium binding changes during the 2line-ferrihydrite alteration process. Environ. Sci. Technol. **36**, 5092 (2002).
8. Denecke, M. A.: Metal-oxygen bond distance determination from XANES spectra, Proceedings of the OECD-NEA workshop on

speciation, techniques and facilities for radioactive materials at synchrotron light sources. Grenoble, France, 4–6 October (1998) p. 135.
9. Withers, S. H., Peale, R. E., Schulte, A. F., Braunstein, G., Beck, K. M., Hess, W. P., Reeder R. J.: Broad distribution of crystal-field environments for Nd^{3+} in calcite. Phys. Chem. Min. **30**, 440 (2003).
10. Elzinga, E. J., Reeder, R. J., Withers, S. H., Peale, R. E., Mason, R. A., Beck, K. M., Hess W. P.: EXAFS study of rare-earth element coordination in calcite. Geochim. Cosmochim. Acta **66**, 2875 (2002).
11. Kim, M. A., Panak, P. J., Yun, J. I., Kim, J. I., Klenze, R., Koehler K.: Interaction of actinides with aluminosilicate colloids in *statu nascendi*: Part I: generation and characterization of actinide(III)-pseudocolloids. Colloid. Surface A **216**, 97 (2003).
12. Kim, M. A., Panak, P. J., Yun, J. I., Priemyshev, A., Kim J. I.: Interaction of actinides(III) with aluminosilicate colloids in *statu nascendi*: Part III. Colloid formation from monosilanol and polysilanol. Colloid. Surface A **254**, 137 (2005).
13. Allen, P. G., Shuh, D. K., Bucher, J. J., Edelstein, N. M., Palmer, C. E. A., Silva, R. J., Nguyen, S. N., Marquez, L. N., Hudson E. A.: Determinations of uranium structures by EXAFS: Schoepite and other U(VI) oxide precipitates. Radiochim. Acta **75**, 47 (1996).
14. Reich, T., Moll, H., Arnold, T., Denecke, M. A., Hennig, C., Geipel, G., Bernhard, G., Nitsche, H., Allen, P. G., Bucher, J. J., Edelstein, N. M., Shuh D. K.: An EXAFS study of uranium(VI) sorption onto silica gel and ferrihydrite. J. Electron. Spectrosc. Relat. Phenom. **96**, 237 (1998).
15. Marquardt, C. M., Seibert, A., Artinger, R., Denecke, M. A., Kuczewski, B., Schild, D., Fanghänel, Th.: The redox behavior of plutonium in humic rich groundwater. Radiochim. Acta **92**, 617 (2004).
16. Rothe, J., Walther, C., Denecke, M. A., Fanghänel, Th.: XAFS and LIBD investigation of the formation and structure of Pu(IV) hydrolysis products. Inorg. Chem. **43**, 4708 (2004).